

# Direct fast method for time-limited signal reconstruction

Yanfei Wang, Zaiwen Wen, Zuhair Nashed, and Qiyu Sun

We consider reconstruction of signals by a direct method for the solution of the discrete Fourier system. We note that the reconstruction of a time-limited signal can be simply realized by using only either the real part or the imaginary part of the discrete Fourier transform (DFT) matrix. Therefore, based on the study of the special structure of the real and imaginary parts of the discrete Fourier matrix, we propose a fast direct method for the signal reconstruction problem, which utilizes the numerically truncated singular value decomposition. The method enables us to recover the original signal in a stable way from the frequency information, which may be corrupted by noise and/or some missing data. The classical inverse Fourier transform cannot be applied directly in the latter situation. The pivotal point of the reconstruction is the explicit computation of the singular value decomposition of the real part of the DFT for any order. Numerical experiments for 1D and 2D signal reconstruction and image restoration are given. © 2006 Optical Society of America

OCIS codes: 070.6020, 070.2580, 100.3010, 100.3020, 100.3190.

## 1. Introduction

Linear systems are one of the important classes of scientific observing systems. An observing system, usually, has an input  $f$  and an output  $F$ , usually corrupted with additive noise  $E$ . The discrete Fourier transform (DFT)  $\mathcal{F}$  is one of the representations of the input-output response. In the ideal case, that is, no noise is added and no data are missing, the discrete Fourier system can be expressed as

$$\begin{bmatrix} 1 & 1 & \cdots & 1 \\ 1 & \omega_N & \cdots & \omega_N^{N-1} \\ \vdots & \vdots & \ddots & \vdots \\ 1 & \omega_N^{N-1} & \cdots & \omega_N^{(N-1)^2} \end{bmatrix} \begin{bmatrix} f_0 \\ f_1 \\ \vdots \\ f_{N-1} \end{bmatrix} = \begin{bmatrix} F_0 \\ F_1 \\ \vdots \\ F_{N-1} \end{bmatrix}, \quad (1.1)$$

where  $\omega_N = \exp(-i(2\pi/N))$ , and  $N$  is the period of the input signal  $f$ . The discrete system (1.1) is related

to a discretization of the integral equation of the first kind (see the Appendix)

$$(Tf)(u) = \int_{-1}^1 \exp(icux)f(x)dx = F(u), \quad (1.2)$$

which arises in many areas of physics and engineering, e.g., Fourier optics,<sup>1</sup> antenna theory,<sup>2-4</sup> object restoration from experimental data,<sup>5-9</sup> Fourier transform spectroscopy<sup>10,11</sup> image extrapolation in optics,<sup>12</sup> and so forth. This integral equation relates to the Fourier transform of a time-limited signal. But unlike the Fourier transform on  $L^2(-\infty, \infty)$ , the finite Fourier transform defined by the operator  $T$  in Eq. (1.2) has unbounded inverse, so the problem of solving Eq. (1.2) for  $f$ , for a given  $F$ , is ill posed.<sup>2</sup> For further details, see the Appendix.

In practical applications, when an input signal passes through the DFT system, some of the frequency information may be lost. The missing of some frequency information is due to the time-domain signal or the space-domain signal passing through a band-limited system. For example, suppose there is a discrete time-limited digital signal  $f$  with period  $N$  and  $N$  components passing through a discrete Fourier system. Suppose that  $M$  samples of the periodic frequency spectrum  $F$  of  $f$  are known. The process can be described as a system of linear algebraic equations

Y. Wang (yfwang\_ucf@yahoo.com) is with the State Key Laboratory of Remote Sensing Science, P.O. Box 9718, Beijing 100101, China. Z. Nashed and Q. Sun, as well as Y. Wang, are with the Department of Mathematics, University of Central Florida, P.O. Box 161364, Orlando, Florida 32816. Z. Wen is with the State Key Laboratory of Scientific and Engineering Computing, Chinese Academy of Sciences, P. O. Box 2719, Beijing 100080, China.

Received 22 February 2005; revised 8 July 2005; accepted 12 September 2005.

0003-6935/06/133111-16\$15.00/0

© 2006 Optical Society of America

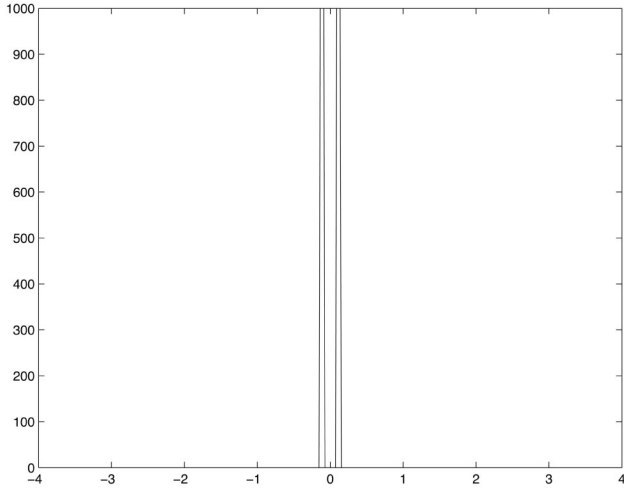


Fig. 1. Input true 1D signal.

$$\sum_{l=0}^{N-1} \omega_N^{kl} f_{l+1} = F_{k+1}, \quad k = 0, 1, \dots, M-1, \quad (1.3)$$

where  $\omega_N = \exp(-i(2\pi/N))$  and

$$f = [f_1, f_2, \dots, f_N]^T, \quad F = [F_1, F_2, \dots, F_M]^T.$$

System (1.3) can be written in a finite rank matrix-vector form:

$$\mathcal{F}f = F, \quad (1.4)$$

where  $F$  is the frequency signal, which can be partially obtained by observation or experiments.

Similar to the above 1D discrete Fourier system, the 2D discrete Fourier system can be described as follows:

$$\mathcal{F}f = \sum_{m=0}^{M-1} \sum_{n=0}^{N-1} \omega_{MN}^{lm, kn} f_{(m+1)(n+1)} = F_{(l+1)(k+1)}, \quad (1.5)$$

where

$$\omega_{MN}^{lm, kn} = \exp[-i2\pi(lm/M + kn/N)],$$

$$l = 0, 1, \dots, M-1; \quad k = 0, 1, \dots, N-1.$$

Here  $\mathcal{F}f$  is a tensor product,  $\mathcal{F} \in \mathbb{R}^{MN \times MN}$ ,  $f \in \mathbb{R}^{MN}$ ,  $F \in \mathbb{R}^{MN}$ . Numerically, we can use the Kronecker multiplication to simplify the computation.

The general problem in the discrete Fourier system is to recover the original signal  $f$  in a stable way from the frequency information  $F$ , which may be corrupted by noise and/or some partial missing data.

In an ideal situation, that is, no noise is added and no data are missing, the widely used method is the inverse fast Fourier transform (IFFT), especially when the total number of sampling points is of the form  $2^k$  for some integer  $k > 0$ .

In general, Eq. (1.4) is overdetermined and the IFFT

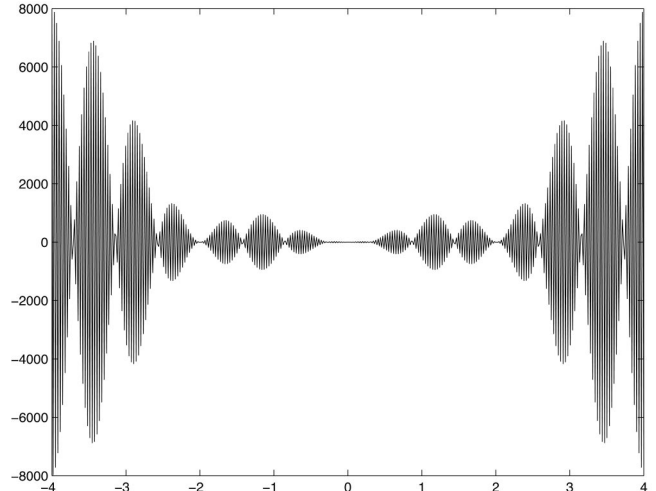


Fig. 2. Exact frequency information.

cannot be employed directly.<sup>13–16</sup> Also, some drawbacks are exhibited, such as in imaging interferometric intensity and phase and/or height.<sup>17</sup> All these difficulties lead to the necessity of resorting to other methods for solving the linear systems (1.4) and (1.5) when the frequency data  $F$  is corrupted and/or partially missing. There are several approaches to the above problem. For instance, the singular value decomposition (SVD) method of the discrete Fourier matrix  $\mathcal{F}$  was introduced for the superresolution<sup>18</sup> and diffraction application<sup>19</sup>; the nonquadratic regularization method of the discrete Fourier system was proposed for the Fourier synthetic aperture radar (SAR) image reconstruction<sup>20</sup> (see also Carrara *et al.*<sup>21</sup> for a comprehensive discussion); and the spectral estimation algorithms were developed for Fourier radar problems.<sup>17,22</sup> Wingham<sup>19</sup> further compared the SVD with Miller's regularization and obtained a least-squares estimation.

The Fourier matrix  $\mathcal{F}$  can be written as

$$\mathcal{F} = \mathcal{F}_r + i\mathcal{F}_i,$$

where  $\mathcal{F}_r$  and  $\mathcal{F}_i$  denote the real and imaginary parts of  $\mathcal{F}$ , respectively. For a time-limited signal, we can simply reconstruct it by either the real or imaginary parts of the DFT system. We use the real part in this paper. Then the input signal is the minimal-norm least-squares solution of the system

$$\mathcal{F}_r f = F_r, \quad (1.6)$$

or

$$f = \mathcal{F}_r^\dagger F_r, \quad (1.7)$$

where the symbol  $\dagger$  denotes the Moore–Penrose generalized inverse. Recall that the Moore–Penrose generalized inverse of a matrix  $A$  is the matrix that assigns to each vector  $y$  the unique minimal-norm least-squares solution of  $Ax = y$ . For theory and com-

computational issues of generalized inverses, particularly the interplay between the continuous and the discrete version; see Ref. 23. Of course we do not compute  $f$  by first computing the generalized inverse and then by multiplying it by  $F_r$ . Rather we compute  $f$  by a numerical method for solving the least-squares problem.<sup>24,25</sup>

We want to point out more about the application of the real or imaginary part of  $\mathcal{F}$  to reconstruct the time-limited signal  $f$ . As is known, the Fourier transform of a time-limited even signal is equivalent to the real part of  $\mathcal{F}$  that applies to  $f$ , whereas the Fourier transform of a time-limited odd signal is equivalent to the imaginary part of  $\mathcal{F}$  that applies to  $f$ . Therefore, if we use Eq. (1.7) as the reconstruction system, it is particularly useful for reconstruction of a time-limited even signal. Nevertheless, any time-limited signal can always be symmetrized to be an even signal.

Now a question that arises immediately is, what about the condition number of  $\mathcal{F}_r$ ? Is the generalized inverse of  $\mathcal{F}_r$  uniformly bounded in  $N$ ? If the condition number of  $\mathcal{F}_r$  is large, then this is a discrete ill-posed problem due to the frequency signal  $F$  containing random noise. For example, we consider a  $10 \times 10$  DFT matrix  $\mathcal{F}_{10 \times 10}$  with entries  $\omega_N^{kn} = \exp(-i(2\pi kn/N))$  and period  $N = 10$ . It is easy to see that the rank of  $\mathcal{F}_r$  is 6 since there are 4 zero singular values and the only nonzero singular value is  $\sqrt{10}$  with algebraic multiplicity 6. But in computer computation, due to the roundoff error and the limit of the machine precision, we can only obtain approximate values of the singular values. So, by using double precision in the computer computation, we get the following singular values of this  $\mathcal{F}_r$ :

$$\sigma_{\text{nonzero}}(\mathcal{F}_r) = \begin{bmatrix} 3.162 & 277 & 660 & 168 & 384 \\ 3.162 & 277 & 660 & 168 & 383 \\ 3.162 & 277 & 660 & 168 & 382 \\ 3.162 & 277 & 660 & 168 & 382 \\ 3.162 & 277 & 660 & 168 & 381 \\ 3.162 & 277 & 660 & 168 & 380 \end{bmatrix},$$

$$\sigma_{\text{nearly zero}}(\mathcal{F}_r) = \begin{bmatrix} 1.945 & 788 & 483 & 288 & 222 \times 10^{-15} \\ 1.253 & 079 & 556 & 056 & 248 \times 10^{-15} \\ 5.263 & 367 & 760 & 387 & 904 \times 10^{-16} \\ 2.198 & 412 & 987 & 245 & 457 \times 10^{-18} \end{bmatrix}.$$

Thus numerically the rank of  $\mathcal{F}_r$  cannot actually be 6 and should be 9 in the computation by regarding the last component of  $\sigma_{\text{nearly zero}}(\mathcal{F}_r)$  as zero. This will cause difficulty for numerical computation. Therefore we introduce the concept of  $\delta$  rank in Section 2 and give a realistic algorithm in Section 3.

To stably recover the original information by Eq. (1.7), some regularization technique should be used. The numerically truncated-singular-value-decomposition (NTSVD) method successfully suppresses the instability induced by the small singular values (see Sec-

tion 3). Moreover, the special properties for  $\mathcal{F}_r$  and  $\mathcal{F}_i$  can be explored more deeply (see Section 4). Our method developed in this paper is based on both of these methods, i.e., we resolve this problem by using the NTSVD. We are able to perform the NTSVD explicitly since in this paper we derive explicit formulas for the singular values and singular vectors for any order  $N$  of the matrix, which is the essence of one of the main contributions of the paper. This is also the pivotal point for the effectiveness of the numerical procedure based on the truncated singular value decomposition (TSVD) analyzed in this paper.

The paper is organized as follows. In Section 2 we recall the SVD method for solving linear DFT system. In Section 3 we present the NTSVD for regularizing the system. In Section 4 we derive explicit SVD formulas for the real and imaginary parts of the Fourier matrix  $\mathcal{F}$ . In Section 5 we give realistic algorithms for 1D and 2D signal reconstruction problems. In Section 6 we present some numerical tests for 1D and 2D signal reconstruction problems from corrupted frequency information. In Section 7 we give a proof for the explicit SVD formulas. In Section 8 we provide conclusions and briefly mention some possible extensions of the proposed method. Finally in the Appendix we reformulate the Fourier transform over a finite interval and state the numerical difficulties due to ill-posedness. We also indicate the particular discretization–collocation scheme that leads to the DFT system (1.1).

Throughout this paper,  $A^T$  and  $A^*$  denote the transpose and conjugate transpose of a matrix  $A$ , respectively,  $I_N$  is the unit matrix of order  $N$ ,  $\|x\|_2 = (\sum_{i=1}^N |x_i|^2)^{1/2}$  is the standard norm of  $x = (x_1, \dots, x_N)^T \in \mathbf{R}^N$ , and  $A(:, s : t)$  denotes the submatrix formed by all rows between  $s$ th and  $t$ th columns of a matrix  $A$ .

## 2. Singular Value Decomposition of the DFT Matrix

Let

$$\mathcal{F} = \begin{bmatrix} 1 & 1 & 1 & \dots & 1 \\ 1 & \omega_N & \omega_N^2 & \dots & \omega_N^{N-1} \\ 1 & \omega_N^2 & \omega_N^4 & \dots & \omega_N^{2(N-1)} \\ \vdots & \vdots & \vdots & \vdots & \vdots \\ 1 & \omega_N^{M-1} & \omega_N^{2(M-1)} & \dots & \omega_N^{(M-1)(N-1)} \end{bmatrix} \in \mathbb{C}^{M \times N} \quad (M > N), \quad (2.1)$$

where  $\omega_N = e^{-i(2\pi/N)}$ . Clearly the entries of  $\mathcal{F}$  consist of  $1, x, x^2, \dots, x^{M-1}$  with  $x = 1, \omega_N, \dots, \omega_N^{N-1}$ . Then

$$\mathcal{F} = \mathcal{F}_r + i\mathcal{F}_i.$$

The entries of  $\mathcal{F}_r$  and  $\mathcal{F}_i$  are  $\cos(2\pi mn/N)$  and  $-\sin(2\pi mn/N)$ , respectively,  $m = 0, 1, \dots, M-1$ , and  $n = 0, 1, \dots, N-1$ .

Let  $F$  represent  $\mathcal{F}_r$  or  $\mathcal{F}_i$ . The SVD of the matrix  $F$  is of the form

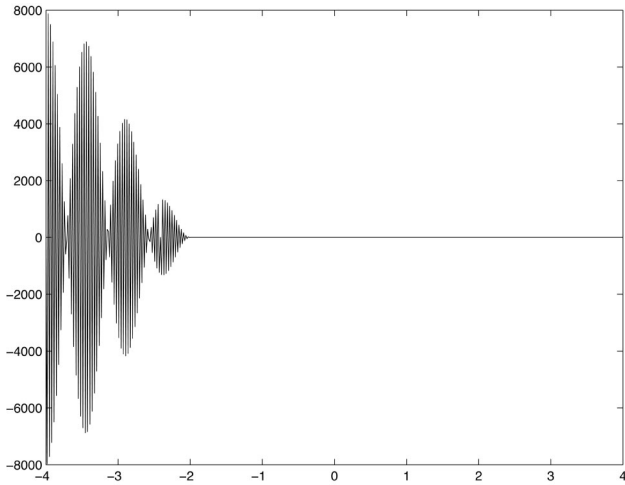


Fig. 3. Noisy, fragmentary frequency.

$$F = U\Sigma V^T = \sum_{i=1}^N \sigma_i u_i v_i^T, \quad (2.2)$$

where  $U = [u_1, u_2, \dots, u_N] \in \mathbb{R}^{M \times N}$  and  $V = [v_1, v_2, \dots, v_N] \in \mathbb{R}^{N \times N}$  are orthonormal matrices,

$$U^T U = V^T V = I_N,$$

$I_N$  is the unit matrix with order  $N$ , and the diagonal matrix  $\Sigma = \text{diag}[\sigma_1, \sigma_2, \dots, \sigma_N]$  satisfies

$$\sigma_1 \geq \sigma_2 \geq \dots \geq \sigma_N.$$

Note that the time-limited signals can be simply reconstructed by using only  $\mathcal{F}_r$ . However, the condition number of  $\mathcal{F}_r$  is large for sufficiently large  $M$  and  $N$  due to its rank deficiency. This causes difficulties in computation, i.e., a small perturbation in  $F$  may lead to large instability in the solution. Moreover, in the presence of errors (machine precision error, measurement errors, discretization errors, etc.), the rigorous

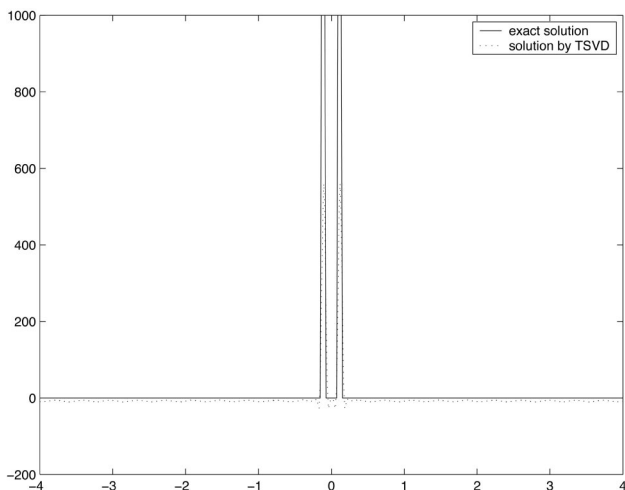


Fig. 4. Reconstructions.

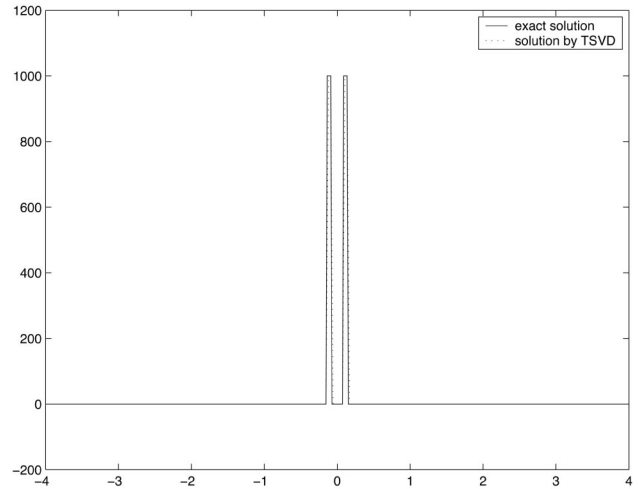


Fig. 5. Reconstructions for the noisy frequency.

definition of the rank is not useful numerically.<sup>26,27</sup> Practically, we introduce the numerical  $\delta$ -rank  $r_\delta$  of a matrix  $A \in \mathbb{R}^{M \times N}$ , with respect to the tolerance  $\delta$ , by

$$r_\delta = \min\{\text{rank}(B_\delta + A) : B_\delta \in \mathbb{R}^{M \times N}, \|B_\delta\|_2 \leq \delta\}.$$

Denote the singular values of  $A$  by  $\sigma_i$  for  $i = 1, 2, \dots, N$ . In terms of the singular values of  $A$ , the numerical  $\delta$ -rank  $r_\delta$  satisfies

$$\sigma_{r_\delta+1} \leq \delta < \sigma_{r_\delta}.$$

When  $A$  is given exactly, then it is natural to choose  $B_\delta$  as the influence of rounding errors during computation of the SVD of  $A$ . Usually  $B_\delta$  is a random matrix with elements from a certain statistical distribution. For example, in image processing,  $B_\delta$  often satisfies the Gaussian distribution with zero mean and standard deviation  $\sigma$  or Poisson distribution with a mean value  $\lambda$ . In view of this, we should not solve the problem by SVD directly; instead we should use some

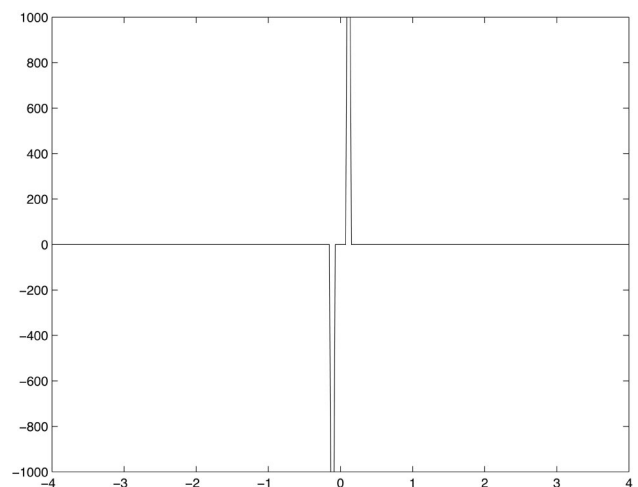


Fig. 6. Input true 1D odd signal.

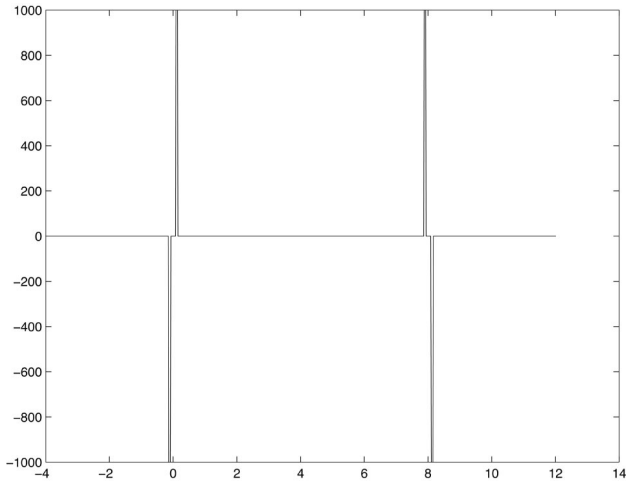


Fig. 7. Symmetrized true 1D odd signal.

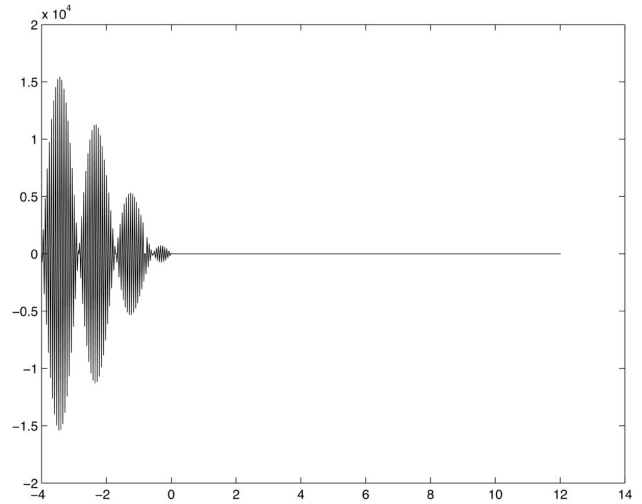


Fig. 9. Noisy, fragmentary frequency.

regularization technique to SVD by taking into account the numerical  $\delta$  rank.

### 3. Numerically Truncated Singular Value Decomposition Method for Least-Squares Problems

Fix an  $M \times N$  matrix  $A$  and a vector  $b \in \mathbb{R}^M$ . Now we consider the following minimization problem:

$$\min_{x \in \mathbb{R}^N} \|Ax - b\|_2. \quad (3.1)$$

Consider the SVD of the matrix  $A$ :

$$A = U\Sigma V^T = \sum_{i=1}^N \sigma_i u_i v_i^T, \quad (3.2)$$

where  $U = [u_1, u_2, \dots, u_N] \in \mathbb{R}^{M \times N}$  and  $V = [v_1, v_2, \dots, v_N] \in \mathbb{R}^{N \times N}$  are orthonormal matrices,

$$U^T U = V^T V = I_N,$$

and the diagonal matrix  $\Sigma = \text{diag}[\sigma_1, \sigma_2, \dots, \sigma_N]$  satisfies

$$|\sigma_1| \geq |\sigma_2| \geq \dots \geq |\sigma_N|.$$

If the rank of  $A$  is  $r$ , then by the SVD of  $A$ , we see that the solution  $x_{LS}$  of the least-squares problem (3.1) of minimal norm is

$$x_{LS} = \sum_{i=1}^r \frac{1}{\sigma_i} (u_i^T b) v_i, \quad (3.3)$$

$$\min_{x \in \mathbb{R}^N} \|Ax - b\|_2^2 = \sum_{i=r+1}^N |u_i^T b|^2.$$

However, in practice,  $A$  may not be exactly rank deficient, but instead numerically rank deficient, i.e., it has one or more small but nonzero singular values such that  $r_\delta < \text{rank}(A)$ . It is clear from (3.3) that the small singular values inevitably give rise to difficul-

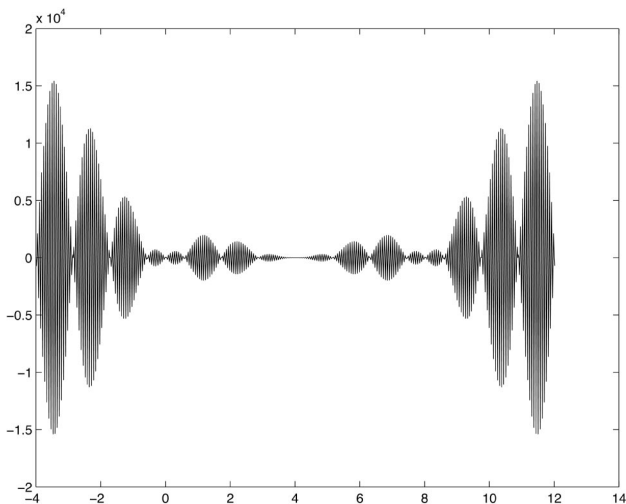


Fig. 8. Exact frequency information for the symmetric case.

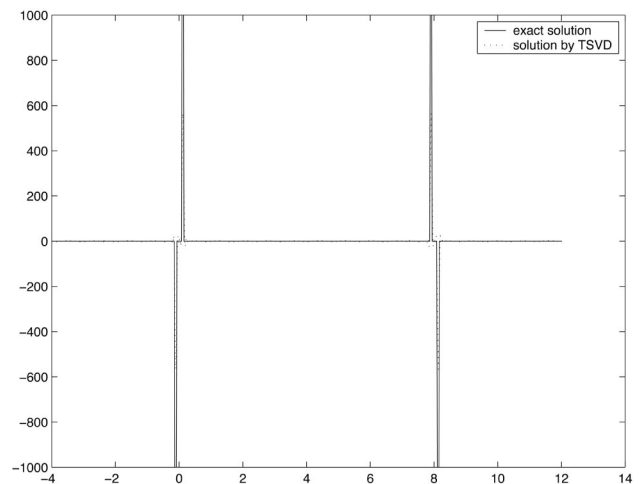


Fig. 10. Reconstructions.

ties. The regularization technique for SVD means some of the small singular values are truncated when in computation, and hence it is called the NTSVD. We apply this technique to the real and imaginary parts of the Fourier matrix. Note that if the Fourier system  $\mathcal{F}$  is corrupted, then so are  $\mathcal{F}_r$  and  $\mathcal{F}_i$ . Now let  $A$  be either  $\mathcal{F}_r$  or  $\mathcal{F}_i$ , and assume that  $A$  is corrupted by the error matrix  $B_\delta$ . Then we replace  $A$  by a matrix  $A_{\tilde{r}}$  that is close to  $A$  and mathematically rank deficient. Our choice of  $A_{\tilde{r}}$  is obtained by replacing the small nonzero singular values  $\sigma_{\tilde{r}+1}, \sigma_{\tilde{r}+2}, \dots, \sigma_N$  with exact zeros, i.e.,

$$A_{\tilde{r}} = \sum_{i=1}^{\tilde{r}} \sigma_i u_i v_i^T, \quad (3.5)$$

where  $\tilde{r}$  is usually chosen as  $r_\delta$ . We call Eq. (3.5) the NTSVD of  $A$ . Now we use Eq. (3.5) instead of the usual SVD (3.2) of the matrix  $A$  to compute the least-squares solutions. Practically, we solve the minimization problem

$$\min_{x \in \mathbb{R}^N} \|A_{\tilde{r}} x - b\|_2, \quad (3.6)$$

instead of Eq. (3.1). In this case, the approximated solution  $x_{\text{LS}}^{\text{appr}}$  of the minimal-norm least-squares problem (3.1) is given by

$$x_{\text{LS}}^{\text{appr}} = A_{\tilde{r}}^\dagger b = \sum_{i=1}^{\tilde{r}} \frac{1}{\sigma_i} (u_i^T b) v_i, \quad (3.7)$$

where  $A_{\tilde{r}}^\dagger$  denotes the Moore–Penrose generalized inverse.

#### 4. Symmetric Case: a Heuristic Approach

In Section 2 we deal with the  $M \times N$  discrete Fourier system  $\mathcal{F}$  when  $M > N$ . However, we can always obtain an  $M \times M$  DFT system by padding  $M-N$  column vectors to the  $M \times N$  discrete Fourier system  $\mathcal{F}$ , and the entries of the extended discrete Fourier system consist of  $1, x, x^2, \dots, x^{M-1}$  with  $x = 1, \omega_M, \dots, \omega_M^{M-1}$ . Correspondingly, padding  $M-N$  zeros to the vector  $f$  does not change the frequency  $F$ .

For example, we can replace Eq. (2.1) by Eq. (4.1) if we pad  $M-N$  zeros following the last component of the vector  $f$ , which does not change the frequency  $F$ . In this way, we obtain the discrete Fourier system in the form

$$\mathcal{F} = \begin{bmatrix} 1 & 1 & 1 & \cdots & 1 \\ 1 & \omega_M & \omega_M^2 & \cdots & \omega_M^{M-1} \\ 1 & \omega_M^2 & \omega_M^4 & \cdots & \omega_M^{2(M-1)} \\ \vdots & \vdots & \vdots & \ddots & \vdots \\ 1 & \omega_M^{M-1} & \omega_M^{2(M-1)} & \cdots & \omega_M^{(M-1)2} \end{bmatrix} \in \mathbb{C}^{M \times M}, \quad (4.1)$$

where  $\omega_M = e^{-i(2\pi/M)}$ . Clearly,  $\mathcal{F}$  is a symmetric matrix, but not Hermitian; the entries of  $\mathcal{F}$  consist of  $1, x, x^2, \dots, x^{M-1}$  with  $x = 1, \omega_M, \dots, \omega_M^{M-1}$ , and  $\mathcal{F}$  satisfies

$$\mathcal{F}^T = \mathcal{F}, \quad \mathcal{F}^* \mathcal{F} = \mathcal{F} \mathcal{F}^* = M I_M, \quad (4.2)$$

where  $I_M$  is the unit matrix of order  $M$ . Moreover, we have the following SVDs for the real and imaginary parts of the Fourier matrix  $\mathcal{F}$ , whose proof is given in Section 7.

**Theorem 4.1.** *Let  $\mathcal{F}_r$  and  $\mathcal{F}_i$  be the real and imaginary parts of the Fourier matrix  $\mathcal{F}$  given in Eq. (4.1). We have the explicit formulas of the SVDs for  $\mathcal{F}_r$  and  $\mathcal{F}_i$ ,*

$$\mathcal{F}_r = U \Sigma_1 V^T, \quad \mathcal{F}_i = U \Sigma_2 V^T, \quad (4.3)$$

where

$$\Sigma_1 = \text{diag} \left( \underbrace{\sqrt{M}, \dots, \sqrt{M}}_r, 0, \dots, 0 \right),$$

$$\Sigma_2 = \text{diag} \left( 0, \dots, 0, \underbrace{\sqrt{M}, \dots, \sqrt{M}}_{M-r} \right).$$

depend on whether  $M$  is even or odd.

(a) For  $M$  even, say  $M = 2p$ , we have  $r = p + 1$  and

$$U = \sqrt{\frac{1}{M}} \begin{bmatrix} 1 & \sqrt{2} & \cdots & \sqrt{2} & 1 & 0 & \cdots & 0 \\ 1 & \sqrt{2}a_1 & \cdots & \sqrt{2}a_{r-2} & a_{r-1} & \sqrt{2}b_{r-2} & \cdots & \sqrt{2}b_1 \\ \vdots & \vdots & \ddots & \vdots & \vdots & \vdots & \ddots & \vdots \\ 1 & \sqrt{2}a_{M-1} & \cdots & \sqrt{2}a_{(M-1)(r-2)} & a_{(r-1)(M-1)} & \sqrt{2}b_{(M-1)(r-2)} & \cdots & \sqrt{2}b_{M-1} \end{bmatrix}, \quad (4.4)$$

$$V = \begin{bmatrix} 1 & 0 & 0 & \cdots & \cdots & \cdots & \cdots & \cdots & 0 & 0 \\ 0 & \frac{\sqrt{2}}{2} & 0 & \cdots & \cdots & \cdots & \cdots & \cdots & 0 & \frac{\sqrt{2}}{2} \\ 0 & 0 & \frac{\sqrt{2}}{2} & \cdots & \cdots & \cdots & \cdots & \cdots & \frac{\sqrt{2}}{2} & 0 \\ \vdots & \vdots & \vdots & \ddots & \vdots & \vdots & \vdots & \vdots & \vdots & \vdots \\ 0 & 0 & 0 & \cdots & \frac{\sqrt{2}}{2} & 0 & \frac{\sqrt{2}}{2} & \cdots & 0 & 0 \\ 0 & 0 & 0 & \cdots & 0 & 1 & 0 & \cdots & 0 & 0 \\ 0 & 0 & 0 & \cdots & \frac{\sqrt{2}}{2} & 0 & -\frac{\sqrt{2}}{2} & \cdots & 0 & 0 \\ \vdots & \vdots & \vdots & \ddots & \vdots & \vdots & \vdots & \ddots & \vdots & \vdots \\ 0 & 0 & \frac{\sqrt{2}}{2} & \cdots & \cdots & \cdots & \cdots & \cdots & -\frac{\sqrt{2}}{2} & 0 \\ 0 & \frac{\sqrt{2}}{2} & 0 & \cdots & \cdots & \cdots & \cdots & \cdots & 0 & -\frac{\sqrt{2}}{2} \end{bmatrix} \quad (p+1)\text{th row}, \quad (4.5)$$

where  $a_k = \cos(2k\pi/M)$  and  $b_k = \sin(2k\pi/M)$  for all positive integers  $k$ . Note that in Eq. (4.5), all the nonzero entries consist of the entries on the main diagonal and on the subdiagonal below the cross diagonal (consisting of zeros).

(b) For  $M$  odd, say  $M = 2p + 1$ , we have  $r = p + 1$  and

where  $a_k$  and  $b_k$  are as in part (a). Note again that in Eq. (4.7) all the nonzero entries consist of the entries on the main diagonal and on the subdiagonal below the cross diagonal.

From Theorem 4.1 we also see that the Fourier matrix  $\mathcal{F}$  can be written as the product of matrices  $U$ ,

$$U = \frac{1}{\sqrt{M}} \begin{bmatrix} 1 & \sqrt{2} & \cdots & \sqrt{2} & 0 & \cdots & 0 \\ 1 & \sqrt{2}a_1 & \cdots & \sqrt{2}a_{r-1} & \sqrt{2}b_{r-1} & \cdots & \sqrt{2}b_1 \\ \vdots & \vdots & \ddots & \vdots & \vdots & \ddots & \vdots \\ 1 & \sqrt{2}a_{M-1} & \cdots & \sqrt{2}a_{(M-1)(r-1)} & \sqrt{2}b_{(M-1)(r-1)} & \cdots & \sqrt{2}b_{M-1} \end{bmatrix}, \quad (4.6)$$

$$V = \begin{bmatrix} 1 & 0 & 0 & \cdots & \cdots & \cdots & \cdots & \cdots & 0 & 0 \\ 0 & \frac{\sqrt{2}}{2} & 0 & \cdots & \cdots & \cdots & \cdots & \cdots & 0 & \frac{\sqrt{2}}{2} \\ 0 & 0 & \frac{\sqrt{2}}{2} & \cdots & \cdots & \cdots & \cdots & \cdots & \frac{\sqrt{2}}{2} & 0 \\ \vdots & \vdots & \vdots & \ddots & \vdots & \vdots & \vdots & \vdots & \vdots & \vdots \\ 0 & 0 & 0 & \cdots & \frac{\sqrt{2}}{2} & \frac{\sqrt{2}}{2} & \cdots & \cdots & 0 & 0 \\ 0 & 0 & 0 & \cdots & \frac{\sqrt{2}}{2} & -\frac{\sqrt{2}}{2} & \cdots & \cdots & 0 & 0 \\ \vdots & \vdots & \vdots & \ddots & \vdots & \vdots & \ddots & \vdots & \vdots & \vdots \\ 0 & 0 & \frac{\sqrt{2}}{2} & \cdots & \cdots & \cdots & \cdots & \cdots & -\frac{\sqrt{2}}{2} & 0 \\ 0 & \frac{\sqrt{2}}{2} & 0 & \cdots & \cdots & \cdots & \cdots & \cdots & 0 & -\frac{\sqrt{2}}{2} \end{bmatrix} \quad (p+1)\text{th row}, \quad (4.7)$$

$V$  and a diagonal matrix  $\Sigma = \Sigma_1 + i\Sigma_2$ ,

$$\mathcal{F} = U\Sigma V^T.$$

It is clear from Theorem 4.1 that  $\mathcal{F}_r$  is a rank-deficient real matrix, that is, its rank is equal to the number of positive singular value of  $\mathcal{F}_r$ . As described in Section 2, this causes difficulties in computation, i.e., a small perturbation in  $F$  may lead to a large instability in the solution. In view of this, we use the TSVD as in Section 3. In solving the minimization problem (3.1) with  $A$  being the perturbation of  $\mathcal{F}_r$ , we let  $r = (M + 2)/2$  when  $M$  is even and  $r = (M + 1)/2$  when  $M$  is odd.

**Remark 4.1.** Note that  $\mathcal{F}_r$  is a symmetric matrix, hence it is unitarily diagonalizable, i.e., there exists an orthogonal matrix  $P(P^{-1} = P^T)$  such that

$$P^{-1}\mathcal{F}_r P = D,$$

where  $D$  is a diagonal matrix whose nonzero entries are the eigenvalues of  $\mathcal{F}_r$  and the columns of  $P$  are orthogonal eigenvectors belonging to the eigenvalues  $\lambda_1, \lambda_2, \dots, \lambda_M$ . Thus the signal  $f$  can be recovered by finding the minimal-norm least-squares solution of the system  $P^T\mathcal{F}_r P f = F$ , i.e.,

$$f = PD^\dagger P^T F,$$

where  $D^\dagger$  is the Moore–Penrose generalized inverse of  $D$ ,

$$D^\dagger = \begin{bmatrix} \lambda_1^{-1} & 0 & \cdots & 0 \\ 0 & \ddots & \ddots & \vdots \\ \vdots & \ddots & \lambda_r^{-1} & 0 \\ 0 & \cdots & 0 & 0 \end{bmatrix},$$

where  $r = \text{rank}(D)$ . However, in general, the matrix  $P$  is a full matrix, so the amount of computation may become excessive for sufficiently large  $N$ . Computations of the singular values and singular vectors of  $\mathcal{F}_r$  turn out to be effective since, as we show in this paper, the matrix  $\mathcal{F}_r^T \mathcal{F}_r$  is *sparse* and moreover we are able to determine explicit formulas for the SVD for any order  $M$ . This result, which in essence is one of the main contributions of the paper, is the pivotal point for the effectiveness of the numerical procedure based on the TSVD analyzed in this paper.

## 5. Applications in Signal Processing

For the general  $M \times N$  ( $M > N$ ) DFT system, we can apply the TSVD method for recovering the input signal  $f$ . As is pointed out in Section 4, any  $M \times N$  ( $M > N$ ) discrete Fourier system  $\mathcal{F}$  can be extended to an  $M \times M$  DFT system where the entries consist of  $1, x, x^2, \dots, x^{M-1}$  with  $x = 1, \omega_M, \dots, \omega_M^{M-1}$ , by padding  $M - N$  column vectors to the  $M \times N$  discrete Fourier system  $\mathcal{F}$ . Therefore we can use the properties in Section 4 to develop some useful algorithms.

### A. 1D Problem

For practical application problems, the frequency information usually contains noise, i.e., instead of  $F_{\text{true}}$ , we may have  $F = F_{\text{true}} + E$ , where  $E$  is an additive noise. If we want to reconstruct the signal  $f$ , we need to solve the following minimization problem:

$$\|E\|_2 \rightarrow \min.$$

This is equivalent to solving the minimization problem

$$J(f) \stackrel{\text{def}}{=} \|\mathcal{F}_r f - F\|_2 \rightarrow \min. \quad (5.1)$$

From Section 4 we find that the SVD of matrices  $\mathcal{F}_r$  can be easily obtained. So let  $\mathcal{F}_r = U\Sigma_1 V^T$  be the SVD of matrix  $\mathcal{F}_r$  determined by Theorem 4.1, where  $U = [u_1, u_2, \dots, u_M]$  and  $V = [v_1, v_2, \dots, v_M]$  are ordered by columns; the solution can be easily obtained by the TSVD.

Based on the above analysis, we give a realistic algorithm for 1D signal reconstruction.

*Algorithm 5.1. Least-squares algorithm for 1D signal reconstruction*

**Step 1.** If  $M$  is even,  $r = M/2 + 1$ , Let  $V = (v_1, v_2, \dots, v_r)$ , Construct  $U = \mathcal{F}_r(:, 1:r)$ ;  $U(:, 2:r-1) = \sqrt{2}U(:, 2:r-1)$ ; Go to Step 3; [Recall that by  $\mathcal{F}_r(:, 1:r)$  we mean the submatrix formed by all rows between the first column and the  $r$ th column].

**Step 2.** If  $M$  is odd,  $r = (M + 1)/2$ , Let  $V = (v_1, v_2, \dots, v_r)$ , Construct  $U = \mathcal{F}_r(:, 1:r)$ ;  $U(:, 2:r) = \sqrt{2}U(:, 2:r)$ ; Go to Step 3;

**Step 3.**  $f_{\text{LS}} = \sum_{i=1}^r (u_i^T F / \sqrt{M}) v_i$ .

**Remark 5.1.** Since both the diagonal matrix  $\Sigma$  and  $V$  are known to be explicitly sparse matrices in advance, therefore the amount of computation for solving Eq. (5.1) lies in the construction of the matrix  $U$  and the computation of  $f_{\text{LS}} = \sum_{i=1}^r (u_i^T F / \sqrt{M}) v_i$ . Let us consider the even nodes  $M$ . The cost for construction of  $U$  is  $O(\frac{1}{2}M^2 - \frac{3}{2}M)$ , and the cost for the computation of  $f_{\text{LS}}$  is  $O(\frac{1}{4}M^2 + \frac{3}{2}M)$ . Thus the total amount of computation for solving Eq. (5.1) is  $O(\frac{3}{4}M^2)$ . This computational effort is much less than other decomposition methods such as LU decomposition, Gauss–Jordan elimination, and the usual SVD and so forth. Similar discussions can be made for 2D time-limited signal reconstruction problems.

### B. 2D Problem

The following definition will be used in analyzing 2D problems that involve the tensor product.

**Definition 5.1.** Given an array  $U \in \mathbb{C}^{M_x \times M_y}$ , one can obtain a vector  $\mathbf{U} \in \mathbb{C}^{M_x M_y}$  by stacking the columns of  $U$ . This defines a linear mapping  $\text{vec}: \mathbb{C}^{M_x \times M_y} \rightarrow \mathbb{C}^{M_x M_y}$ ,

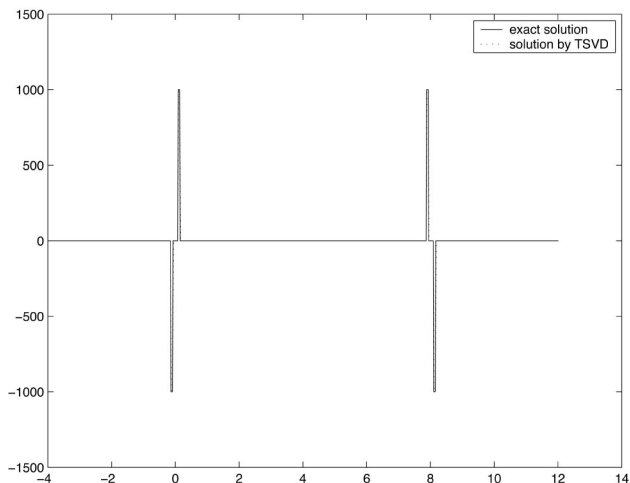


Fig. 11. Reconstructions for the noisy frequency.

$$\text{vec}(U) = [U_{11}, \dots, U_{M_x1}, U_{12}, \dots, U_{M_x2}, \dots, U_{1M_y}, \dots, U_{M_xM_y}]^T.$$

This corresponds to lexicographical column ordering of the elements in the array  $U$ .

For a 2D problem, the computation process is a little more complex than the 1D problem. However, by employing the Kronecker product, we can still find an easy way to reconstruct the original signal.

Let  $\mathcal{F}_x = A_x + B_x i$ ,  $\mathcal{F}_y = A_y + B_y i$ ,  $M_x = \dim(\mathcal{F}_x)$ ,  $M_y = \dim(\mathcal{F}_y)$ ,  $r_x = \text{rank}(A_x)$ , and  $r_y = \text{rank}(A_y)$ . Then

$$\begin{aligned} \mathcal{F}_x \otimes \mathcal{F}_y &= (A_x + B_x i) \otimes (A_y + B_y i) \\ &= (A_x \otimes A_y - B_x \otimes B_y) \\ &\quad + (A_x \otimes B_y - B_x \otimes A_y)i. \end{aligned}$$



Fig. 12. Input true 2D signal.

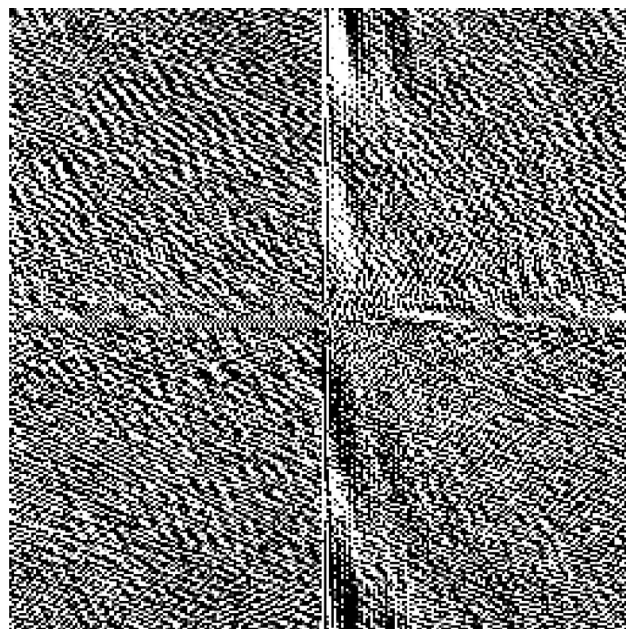


Fig. 13. Exact frequency information.

The 2D minimization problem is in the form

$$\min \|\mathcal{H}\mathbf{f} - \mathbf{F}\|_2, \quad (5.2)$$

where  $\mathcal{H} = \text{real}(\mathcal{F}_x \otimes \mathcal{F}_y)$ ,  $\mathbf{f} = \text{vec}(f)$ , and  $\mathbf{F} = \text{vec}(F)$ . From Theorem 4.1, we have

$$\begin{aligned} A_x &= U_x \begin{bmatrix} \Sigma_{1x} & 0 \\ 0 & 0 \end{bmatrix} V_x^T, & A_y &= U_y \begin{bmatrix} \Sigma_{1y} & 0 \\ 0 & 0 \end{bmatrix} V_y^T, \\ B_x &= U_x \begin{bmatrix} 0 & 0 \\ 0 & \Sigma_{2x} \end{bmatrix} V_x^T, & B_y &= U_y \begin{bmatrix} 0 & 0 \\ 0 & \Sigma_{2y} \end{bmatrix} V_y^T, \end{aligned}$$

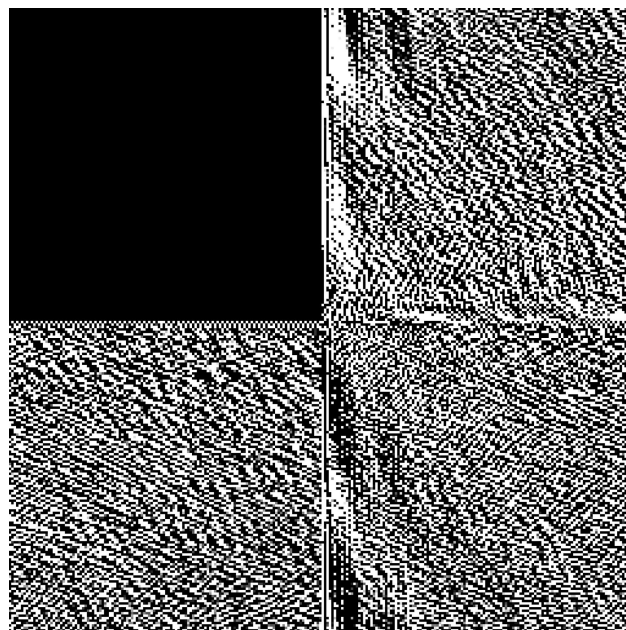


Fig. 14. Noisy, fragmentary frequency.



Fig. 15. Reconstructions.

where  $\Sigma_{1x} = \sqrt{M_x}I_{r_x}$ ,  $\Sigma_{2x} = \sqrt{M_x}I_{M_x-r_x}$ ,  $\Sigma_{1y} = \sqrt{M_y}I_{r_y}$ , and  $\Sigma_{2y} = \sqrt{M_y}I_{M_y-r_y}$ . So

$$\begin{aligned} \mathcal{H} &= A_x \otimes A_y - B_x \otimes B_y \\ &= (U_x \otimes U_y) \Sigma (V_x \otimes V_y)^T, \end{aligned} \quad (5.3)$$

where

$$\Sigma = \begin{bmatrix} \Sigma_{1x} & 0 \\ 0 & 0 \end{bmatrix} \otimes \begin{bmatrix} \Sigma_{1y} & 0 \\ 0 & 0 \end{bmatrix} - \begin{bmatrix} 0 & 0 \\ 0 & \Sigma_{2x} \end{bmatrix} \otimes \begin{bmatrix} 0 & 0 \\ 0 & \Sigma_{2y} \end{bmatrix}.$$

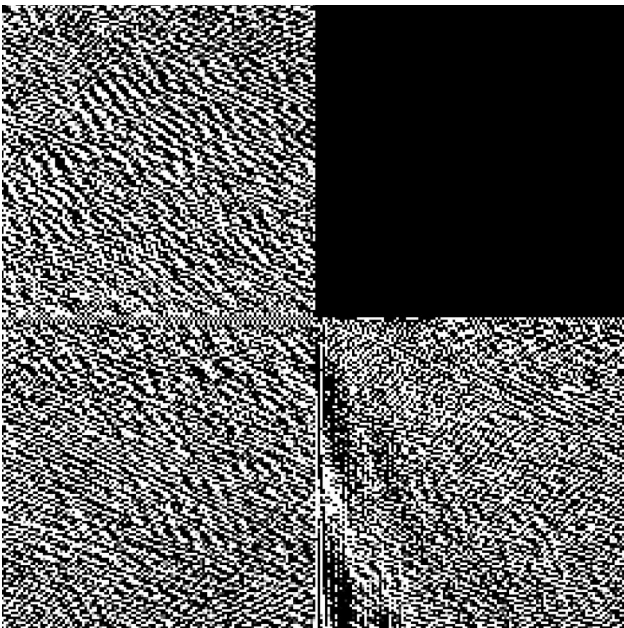


Fig. 16. Noisy, fragmentary frequency.

From the discussion in Section 3, the least-squares solution of minimal norm can be represented in the following form:

$$\mathbf{f}_{LS} = \mathcal{H}^\dagger \mathbf{F} = (V_x \otimes V_y) \Sigma^\dagger (U_x \otimes U_y)^T \mathbf{F}, \quad (5.4)$$

where  $\Sigma^\dagger$  is in the form

$$\begin{aligned} \Sigma^\dagger &= \begin{bmatrix} \Sigma_{1x}^{-1} & 0 \\ 0 & 0 \end{bmatrix} \otimes \begin{bmatrix} \Sigma_{1y}^{-1} & 0 \\ 0 & 0 \end{bmatrix} \\ &\quad - \begin{bmatrix} 0 & 0 \\ 0 & \Sigma_{2x}^{-1} \end{bmatrix} \otimes \begin{bmatrix} 0 & 0 \\ 0 & \Sigma_{2y}^{-1} \end{bmatrix}. \end{aligned}$$

By definition 5.1, we can expand (5.4) as

$$(U_x \otimes U_y)^T \mathbf{F} = \text{vec}(U_y^T F U_x) = \text{vec}(F')$$

and

$$\begin{aligned} \Sigma^\dagger \text{vec}(F') &= \text{vec} \left( \begin{bmatrix} \Sigma_{1y}^{-1} & 0 \\ 0 & 0 \end{bmatrix} F' \begin{bmatrix} \Sigma_{1x}^{-1} & 0 \\ 0 & 0 \end{bmatrix} \right. \\ &\quad \left. - \begin{bmatrix} 0 & 0 \\ 0 & \Sigma_{2y}^{-1} \end{bmatrix} F' \begin{bmatrix} 0 & 0 \\ 0 & \Sigma_{2x}^{-1} \end{bmatrix} \right) \\ &= \text{vec} \left( \begin{bmatrix} F_1'' & 0 \\ 0 & -F_2'' \end{bmatrix} \right) = \text{vec}(F''), \end{aligned} \quad (5.5)$$

where

$$F_1'' = U_{1y}^T F U_{1x} / \sqrt{M_x M_y}, \quad F_2'' = U_{2y}^T F U_{2x} / \sqrt{M_x M_y},$$

and  $U_{1x}$  is the first  $r_x$  columns of  $U_x$ ,  $U_{2x}$  is the last  $M_x - r_x$  columns of  $U_x$ , and  $U_{1y}$ ,  $U_{2y}$ ,  $V_{1x}$ ,  $V_{2x}$ ,  $V_{1y}$ ,  $V_{2y}$ , and so on.

We also note that

$$\begin{aligned} (V_x \otimes V_y) \text{vec}(F'') &= \text{vec} \left( V_y \begin{bmatrix} F_1'' & 0 \\ 0 & -F_2'' \end{bmatrix} V_x^T \right) \\ &= \text{vec} \left( [V_{1y} \ V_{2y}] \begin{bmatrix} F_1'' & 0 \\ 0 & -F_2'' \end{bmatrix} \right. \\ &\quad \left. \times [V_{1x} \ V_{2x}]^T \right) \\ &= \text{vec}(V_{1y} F_1'' V_{1x}^T - V_{2y} F_2'' V_{2x}^T). \end{aligned} \quad (5.6)$$

Hence

$$\mathbf{f}_{LS} = \text{vec}(V_{1y} F_1'' V_{1x}^T - V_{2y} F_2'' V_{2x}^T). \quad (5.7)$$

The above analysis yields an efficient algorithm for 2D signal reconstruction.

*Algorithm 5.2. Least-squares algorithm for 2D signal reconstruction*

Construct  $U_x$ ,  $V_x$ ,  $U_y$ ,  $V_y$  as in Theorem 4.1;



Fig. 17. Reconstructions.

$$F_1'' = U_{1y}^T F U_{1x} / \sqrt{M_x M_y};$$

$$F_2'' = U_{2y}^T F U_{2x} / \sqrt{M_x M_y};$$

$$\mathbf{f}_{LS} = \text{vec}(V_{1y} F_1'' V_{1x}^T - V_{2y} F_2'' V_{2x}^T).$$

## 6. Numerical Tests

In this section we give two examples for 1D or 2D signal reconstructions to demonstrate the effectiveness of the NTSVD method for recovering information.

### Example 6.1. 1D Two Pulse Signal Reconstruction

In this example we consider a 1D signal reconstruction problem, which is also discussed by Gerchberg<sup>28</sup>. The input signal is given by

$$f(x) = 1000 \left[ \text{rect} \left( 16 \left( x - \frac{3.5}{32} \right) \right) + \text{rect} \left( 16 \left( x + \frac{3.5}{32} \right) \right) \right], \quad (6.1)$$

in which the signal consisted of two pulses each  $\frac{1}{16}$  unit long (two samples per pulse), symmetrically placed about the origin and separated by a length of  $\frac{7}{32}$  units. The pulses were 1000 units high and in phase. Numerically, we define the signal  $f(t)$  in  $[-4, 4]$ . The function  $f$  is approximated by a discrete vector  $\mathbf{f}$  with  $M = 500$  sampling points. Here  $\mathbf{f}$  is a discretization of the function  $f$ .

In our numerical test, the frequency information  $\mathbf{F}$  of the original signal  $f$  is obtained by passing through the discrete Fourier system with Gaussian noise added, i.e.,

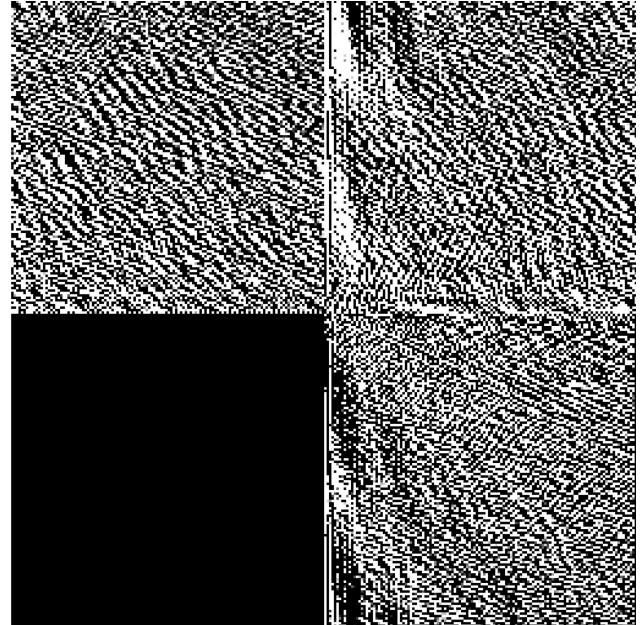


Fig. 18. Noisy, fragmentary frequency.

$$\mathbf{F} : = \mathbf{F}_{\text{noise}} = \mathbf{F}_{\text{true}} + \text{rand}(\text{size}(\mathbf{F}_{\text{true}})),$$

where  $\text{rand}(\cdot)$  represents the Gaussian noise function and  $\text{size}(\cdot)$  represents that the dimension of  $\mathbf{F}_{\text{noise}}$  is the same as  $\mathbf{F}_{\text{true}}$ . The signal-to-noise ratio (SNR) is 37.32 dB.

The true 1D signal and its frequency information are plotted in Figs. 1 and 2, respectively, while the reconstruction figure via the NTSVD method is plotted as in Fig. 5. From Fig. 5, we see that the shape of the reconstructed signal is not too much affected by noise. The reason for this phenomenon, we believe, is that the error propagation is successfully suppressed by the NTSVD, i.e., the small singular values play a minor role in the numerical computation.

To simulate the practical applications and to demonstrate the advantage of the NTSVD method, we consider the signal reconstruction problem in case the frequency data are severely damaged. For instance, some parts of the frequency information  $\mathbf{F}$  are missing or undetected due to various reasons. Figure 3 is the noisy, fragmentary frequency information with some missing frequency data that are replaced by zero,  $\mathbf{F}(1) = 0$ ,  $\mathbf{F}(N/5) = 0$ ,  $\mathbf{F}(N/4 + 1 : N) = 0$ , while Fig. 4 is the original signal (solid curve) and the reconstruction signal (dashed curve) obtained from the NTSVD method in this paper. Here the notation  $\mathbf{F}(N/4 + 1 : N) = 0$  means that the vector is formed by replacing all rows between  $N/4 + 1$  and  $N$  [including the  $(N/4 + 1)$ th row and the  $N$ th row] with zeros. From Fig. 4 we see that the reconstructed signal has almost the same shape as the original one. Comparing Fig. 5 with Fig. 4, we find that the reconstructions are not too much affected by noise but are much more dependent on the quality of the frequency information. We note that this example provides a symmetric



Fig. 19. Reconstructions.

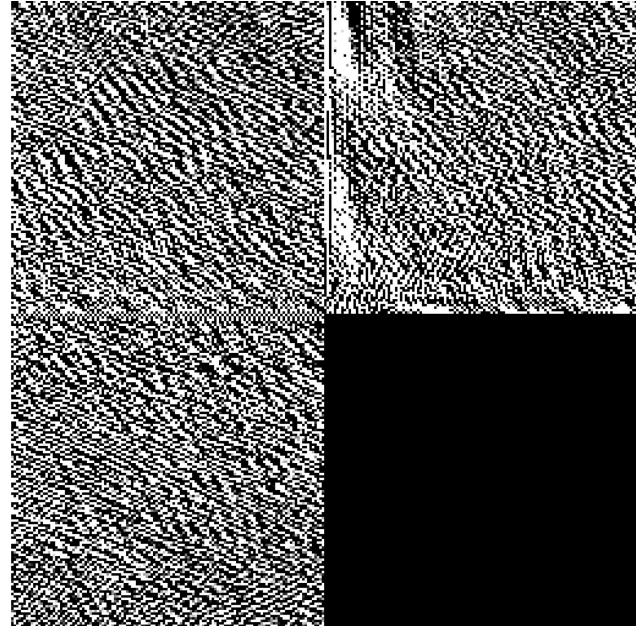


Fig. 20. Noisy, fragmentary frequency.

time-limited signal. This is equivalent to saying that only the real part of the Fourier matrix plays a role in the reconstruction. Actually, any time-limited signal can be symmetrized. For example, suppose the input signal is

$$f(x) = 1000 \left[ \text{rect} \left( 16 \left( x - \frac{3.5}{32} \right) \right) - \text{rect} \left( 16 \left( x + \frac{3.5}{32} \right) \right) \right], \quad (6.2)$$

which is an odd signal, then its symmetric form can be obtained by

$$f(x) = \begin{cases} 1000 \text{rect} \left( 16 \left( x - \frac{3.5}{32} \right) \right) - 1000 \text{rect} \left( 16 \left( x + \frac{3.5}{32} \right) \right) & \text{for } x \in [-4, 4], \\ 1000 \text{rect} \left( 16 \left( x + \frac{3.5}{32} \right) \right) - 1000 \text{rect} \left( 16 \left( x - \frac{3.5}{32} \right) \right) & \text{for } x \in [4, 12]. \end{cases} \quad (6.3)$$

Therefore the recovery process is the same as in the even signal. The simulation results are shown in Figs. 6–11 with similar captions as in the even signal.

Note that the symmetrization of a time-limited signal leads to only a slight increase in the computational cost in the numerical implementation, since in Remark 5.1 we have shown that the total amount of computation for solving Eq. (5.1) is  $O(\frac{3}{4}M^2)$ . Therefore, for a symmetrized signal with  $2M$  points, the cost

would be  $O(3M^2)$ . This computational cost is quite reasonable for modern computers.

#### Example 6.2. Photoimage Restoration

In this example we consider a 2D signal reconstruction problem: photoimage restoration. The original image is the widely used  $256 \times 256$  photo “Lena.” See Figs. 12 and 13 for the original image and its frequency spectrum, respectively. Numerically, image  $f$  is approximated by a discrete vector  $\mathbf{f}$  with  $M_x = M_y = 2^8$  sampling points.

The frequency information  $\mathbf{F}$  is obtained by a procedure similar to the one as shown in Example 6.1:

passing the discrete Fourier system to get the output  $\mathbf{F}_{\text{true}}$ , adding Gaussian white noise to  $\mathbf{F}_{\text{true}}$  with a SNR level of 32.81 dB, and replacing the partial frequency information by zero (that is, those parts of the frequency information that are missing). We assume that the frequencies of the four quadrants are lost one by one. Figure 12 is a plot of the original 2D signal; Fig. 13 is a plot of its frequency spectrum. Figures 14–21 are the plots of the noisy, fragmentary frequency information and the corresponding reconstructions via the NTSVD method. Note that for

visualizing the frequency information more clearly, we swap the first and third quadrants and the second and fourth quadrants. From Figs. 14–19 we observe that the image is not damaged much and most of the details are preserved. Figures 20 and 21 indicate that the fourth quadrant of the shifted frequency plays a more important role than others in the quality of reconstruction.

**7. Proof of Theorem 4.1**

For proof of the theorem, we need the following lemmas.

**Lemma 7.1.** Suppose  $\mathcal{F} \in \mathbb{C}^{M \times M}$  is the Fourier matrix, and let  $\mathcal{H}_r := \mathcal{F}_r^T \mathcal{F}_r$  and  $\mathcal{H}_i := \mathcal{F}_i^T \mathcal{F}_i$ . Then

(1) If  $M$  is even, then

$$\mathcal{H}_r = \begin{bmatrix} M & 0 & 0 & \cdots & \cdots & \cdots & \cdots & \cdots & 0 & 0 \\ 0 & \frac{M}{2} & 0 & \cdots & \cdots & \cdots & \cdots & \cdots & 0 & \frac{M}{2} \\ 0 & 0 & \frac{M}{2} & \cdots & \cdots & \cdots & \cdots & \cdots & \frac{M}{2} & 0 \\ \vdots & \vdots & \vdots & \ddots & \vdots & \vdots & \vdots & \vdots & \vdots & \vdots \\ 0 & 0 & 0 & \cdots & \frac{M}{2} & 0 & \frac{M}{2} & \cdots & 0 & 0 \\ 0 & 0 & 0 & \cdots & 0 & M & 0 & \cdots & 0 & 0 \\ 0 & 0 & 0 & \cdots & \frac{M}{2} & 0 & \frac{M}{2} & \cdots & 0 & 0 \\ \vdots & \vdots & \vdots & \ddots & \vdots & \vdots & \vdots & \ddots & \vdots & \vdots \\ 0 & 0 & \frac{M}{2} & \cdots & \cdots & \cdots & \cdots & \cdots & \frac{M}{2} & 0 \\ 0 & \frac{M}{2} & 0 & \cdots & \cdots & \cdots & \cdots & \cdots & 0 & \frac{M}{2} \end{bmatrix} \times (p+1)\text{th row,} \tag{7.1}$$

$$\mathcal{H}_i = \begin{bmatrix} 0 & 0 & 0 & \cdots & \cdots & \cdots & \cdots & \cdots & 0 & 0 \\ 0 & \frac{M}{2} & 0 & \cdots & \cdots & \cdots & \cdots & \cdots & 0 & -\frac{M}{2} \\ 0 & 0 & \frac{M}{2} & \cdots & \cdots & \cdots & \cdots & \cdots & -\frac{M}{2} & 0 \\ \vdots & \vdots & \vdots & \ddots & \vdots & \vdots & \vdots & \vdots & \vdots & \vdots \\ 0 & 0 & 0 & \cdots & \frac{M}{2} & 0 & -\frac{M}{2} & \cdots & 0 & 0 \\ 0 & 0 & 0 & \cdots & 0 & 0 & 0 & \cdots & 0 & 0 \\ 0 & 0 & 0 & \cdots & -\frac{M}{2} & 0 & \frac{M}{2} & \cdots & 0 & 0 \\ \vdots & \vdots & \vdots & \ddots & \vdots & \vdots & \vdots & \ddots & \vdots & \vdots \\ 0 & 0 & -\frac{M}{2} & \cdots & \cdots & \cdots & \cdots & \cdots & \frac{M}{2} & 0 \\ 0 & -\frac{M}{2} & 0 & \cdots & \cdots & \cdots & \cdots & \cdots & 0 & \frac{M}{2} \end{bmatrix} \times (p+1)\text{th row} \tag{7.2}$$

(2) If  $M$  is odd, then

$$\mathcal{H}_r = \begin{bmatrix} M & 0 & 0 & \cdots & \cdots & \cdots & \cdots & \cdots & 0 & 0 \\ 0 & \frac{M}{2} & 0 & \cdots & \cdots & \cdots & \cdots & \cdots & 0 & \frac{M}{2} \\ 0 & 0 & \frac{M}{2} & \cdots & \cdots & \cdots & \cdots & \cdots & \frac{M}{2} & 0 \\ \vdots & \vdots & \vdots & \ddots & \vdots & \vdots & \vdots & \vdots & \vdots & \vdots \\ 0 & 0 & 0 & \cdots & \frac{M}{2} & \frac{M}{2} & \cdots & \cdots & 0 & 0 \\ 0 & 0 & 0 & \cdots & \frac{M}{2} & \frac{M}{2} & \cdots & \cdots & 0 & 0 \\ \vdots & \vdots & \vdots & \ddots & \vdots & \vdots & \ddots & \vdots & \vdots & \vdots \\ 0 & 0 & \frac{M}{2} & \cdots & \cdots & \cdots & \cdots & \cdots & \frac{M}{2} & 0 \\ 0 & \frac{M}{2} & 0 & \cdots & \cdots & \cdots & \cdots & \cdots & 0 & \frac{M}{2} \end{bmatrix} (p+1)\text{th row,} \tag{7.3}$$

$$\mathcal{H}_i = \begin{bmatrix} 0 & 0 & 0 & \cdots & \cdots & \cdots & \cdots & \cdots & 0 & 0 \\ 0 & \frac{M}{2} & 0 & \cdots & \cdots & \cdots & \cdots & \cdots & 0 & -\frac{M}{2} \\ 0 & 0 & \frac{M}{2} & \cdots & \cdots & \cdots & \cdots & \cdots & -\frac{M}{2} & 0 \\ \vdots & \vdots & \vdots & \ddots & \vdots & \vdots & \vdots & \vdots & \vdots & \vdots \\ 0 & 0 & 0 & \cdots & \frac{M}{2} & -\frac{M}{2} & \cdots & \cdots & 0 & 0 \\ 0 & 0 & 0 & \cdots & -\frac{M}{2} & \frac{M}{2} & \cdots & \cdots & 0 & 0 \\ \vdots & \vdots & \vdots & \ddots & \vdots & \vdots & \ddots & \vdots & \vdots & \vdots \\ 0 & 0 & -\frac{M}{2} & \cdots & \cdots & \cdots & \cdots & \cdots & \frac{M}{2} & 0 \\ 0 & -\frac{M}{2} & 0 & \cdots & \cdots & \cdots & \cdots & \cdots & 0 & \frac{M}{2} \end{bmatrix} (p+1)\text{th row.} \tag{7.4}$$

*Proof.* Consider a unit circle that is partitioned into  $N$  equal arcs with the nodes  $\theta_l = 2kl\pi/M$ ,  $l = 0, 2, \dots, M-1$ . Note that  $\cos \theta_l$  is the projection onto the  $x$  axis of the vector extending from the center of the unit circle to the point  $(\cos \theta_l, \sin \theta_l)$ , where  $\sin \theta_l$  is the projection onto the  $y$  axis. Therefore the following equalities can be easily obtained:

$$\sum_{l=0}^{M-1} \cos \frac{2kl\pi}{M} \cos \frac{2k'l\pi}{M} = \sum_{l=0}^{M-1} \sin \frac{2kl\pi}{M} \sin \frac{2k'l\pi}{M} = 0 \tag{7.5}$$

for all integers  $k, k'$  with  $k \pm k' \notin M\mathbf{Z}$ ,

$$\sum_{l=0}^{M-1} \cos^2 \frac{2kl\pi}{M} = \sum_{l=0}^{M-1} \sin^2 \frac{2kl\pi}{M} = \frac{M}{2} \tag{7.6}$$

for all  $k \in \mathbf{Z}$  with  $2k \notin M\mathbf{Z}$ , and

$$\sum_{l=0}^{M-1} \cos \frac{2kl\pi}{M} \sin \frac{2k'l\pi}{M} = 0 \quad (7.7)$$

for all integers  $k, k'$ . These relationships directly lead to (1) and (2) for even  $M$  and odd  $M$ , respectively.  $\square$

**Lemma 7.2.** The eigenvalue decompositions of  $\mathcal{H}_r$  and  $\mathcal{H}_i$  are given by

$$\mathcal{H}_r = V^T \Lambda_1 V, \quad \mathcal{H}_i = V^T \Lambda_2 V,$$

where  $\Lambda_1 = \text{diag}(M, \dots, M, 0, \dots, 0)$  and  $\Lambda_2 =$

$\text{diag}(0, \dots, 0, \overbrace{M, \dots, M}^r)$ . The matrix  $V$  is orthogo-

nal, i.e.,  $V^T V = I$  and is in the form

$$V = \begin{bmatrix} 1 & 0 & 0 & \cdots & \cdots & \cdots & \cdots & \cdots & 0 & 0 \\ 0 & \frac{\sqrt{2}}{2} & 0 & \cdots & \cdots & \cdots & \cdots & \cdots & 0 & \frac{\sqrt{2}}{2} \\ 0 & 0 & \frac{\sqrt{2}}{2} & \cdots & \cdots & \cdots & \cdots & \cdots & \frac{\sqrt{2}}{2} & 0 \\ \vdots & \vdots & \vdots & \ddots & \vdots & \vdots & \vdots & \vdots & \vdots & \vdots \\ 0 & 0 & 0 & \cdots & \frac{\sqrt{2}}{2} & 0 & \frac{\sqrt{2}}{2} & \cdots & 0 & 0 \\ 0 & 0 & 0 & \cdots & 0 & 1 & 0 & \cdots & 0 & 0 \\ 0 & 0 & 0 & \cdots & \frac{\sqrt{2}}{2} & 0 & -\frac{\sqrt{2}}{2} & \cdots & 0 & 0 \\ \vdots & \vdots & \vdots & \ddots & \vdots & \vdots & \vdots & \ddots & \vdots & \vdots \\ 0 & 0 & \frac{\sqrt{2}}{2} & \cdots & \cdots & \cdots & \cdots & \cdots & -\frac{\sqrt{2}}{2} & 0 \\ 0 & \frac{\sqrt{2}}{2} & 0 & \cdots & \cdots & \cdots & \cdots & \cdots & 0 & -\frac{\sqrt{2}}{2} \end{bmatrix} \times (p+1)\text{th row} \quad (7.8)$$

for even  $M$  and

$$V = \begin{bmatrix} 1 & 0 & 0 & \cdots & \cdots & \cdots & \cdots & \cdots & 0 & 0 \\ 0 & \frac{\sqrt{2}}{2} & 0 & \cdots & \cdots & \cdots & \cdots & \cdots & 0 & \frac{\sqrt{2}}{2} \\ 0 & 0 & \frac{\sqrt{2}}{2} & \cdots & \cdots & \cdots & \cdots & \cdots & \frac{\sqrt{2}}{2} & 0 \\ \vdots & \vdots & \vdots & \ddots & \vdots & \vdots & \vdots & \vdots & \vdots & \vdots \\ 0 & 0 & 0 & \cdots & \frac{\sqrt{2}}{2} & \frac{\sqrt{2}}{2} & \cdots & \cdots & 0 & 0 \\ 0 & 0 & 0 & \cdots & \frac{\sqrt{2}}{2} & -\frac{\sqrt{2}}{2} & \cdots & \cdots & 0 & 0 \\ \vdots & \vdots & \vdots & \ddots & \vdots & \vdots & \ddots & \vdots & \vdots & \vdots \\ 0 & 0 & \frac{\sqrt{2}}{2} & \cdots & \cdots & \cdots & \cdots & \cdots & -\frac{\sqrt{2}}{2} & 0 \\ 0 & \frac{\sqrt{2}}{2} & 0 & \cdots & \cdots & \cdots & \cdots & \cdots & 0 & -\frac{\sqrt{2}}{2} \end{bmatrix} \times (p+1)\text{th row} \quad (7.9)$$

for odd  $M$ , where  $r = (M + 2)/2$  for even  $M$  and  $r = (M + 1)/2$  for odd  $M$ .

*Proof.* We will only discuss Fourier matrix of even order. Let  $\det(C)$  denote the determinant of a square matrix  $C$ . It is easy to show

$$\det(\mathcal{H}_r - \lambda I) = (-\lambda)^{M/2-1} (M - \lambda)^{M/2+1}. \quad (7.10)$$

Thus the distinct eigenvalues of  $\mathcal{H}_r$  are  $N$  and  $0$ . Furthermore, one can easily determine the corresponding orthonormal eigenvectors (7.8) by construction.  $\square$

#### Proof of Theorem 4.1

*Proof.* Suppose  $\mathcal{F}_r = U \Sigma_1 V^T$ , then  $\mathcal{F}_r^T \mathcal{F}_r = V \Sigma_1^2 V^T$  is an eigenvalue decomposition. From Lemma 7.2, we see

$$\Sigma_1 = \text{diag} \left( \underbrace{\sqrt{M}, \dots, \sqrt{M}}_r, 0, \dots, 0 \right),$$

and obviously  $V$  can be taken as Eq. (7.8) or (7.9), respectively. Once  $V$  is determined, the first  $r$  columns of  $U$  can be easily established by relationship  $\mathcal{F}_r V = U \Sigma_1$  due to the nonzero singular values. The remaining columns can just be taken as vectors orthogonal to the first  $r$  columns. Note  $\mathcal{F}_r^T \mathcal{F}_i = 0^0$ , thus we get  $U$  as Eq. (4.4) or (4.6) for even  $M$  and odd  $M$ , respectively.  $\square$

#### 8. Discussion and Conclusion

We have proposed a NTSVD algorithm for recovering information through the Fourier system. The algorithm is based on the study of the special structure of the real and imaginary parts of the discrete Fourier matrix  $\mathcal{F}$ .

The TSVD method is applicable when the system is overdetermined, since in such a case the solution of a least-squares problem is inevitable. This method is also useful for radar problems<sup>16,20,21</sup> and medical image processing problems, such as magnetic resonance imaging (MRI), computerized tomography, and magnetic resonance spectroscopic imaging.<sup>13</sup> Because this kind of problem involves selection of observations, it may be expensive and sometimes dangerous.

Our algorithms are also applicable for the case of nonuniform nodes  $F_k$ ,  $k = 1, 2, \dots$ . In such a case, in order to recover  $f$ , a simple way is to interpolate first the right-hand side  $F$  to form a new vector  $\mathbf{F}$  with equidistant entries, then apply our algorithm to  $\mathbf{F}$ . Finally, we determine the solution by memorizing the locations of the original signal.

#### Appendix: the Fourier Transform over a Finite Interval

Consider the integral operator  $T$  defined by Eq. (1.2) on the space  $L^2[-1, 1]$  of all square-integrable functions (finite energy signals on  $[-1, 1]$ ). The results of Slepian and Pollak<sup>12</sup> guarantee the existence of a complete set of real eigenfunctions  $\{\psi_j\}_{j=0}^\infty$  for the integral operator and a corresponding decreasing sequence of real positive eigenvalues  $\{\lambda_j\}_{j=0}^\infty$ . Indeed,

the eigenfunction  $\psi_n$  is identified as the angular prolate spheroidal function of order  $n$  while the corresponding  $\lambda_n$  is the value of the radial prolate spheroidal function of the same order evaluated at 1 (with our normalization). Moreover, the eigenfunctions satisfy the orthogonality condition

$$\int_{-1}^1 \psi_i(t)\psi_j(t)dt = \begin{cases} 0, & i \neq j, \\ \frac{2\pi}{c}\lambda_i^2, & i = j. \end{cases}$$

The completeness of these functions in  $L^2[-1, 1]$  guarantees that the range of the operator defined by Eq. (1.2) is dense in this space.

Again, the results of Slepian and Pollak<sup>12</sup> show that the eigenfunction  $\psi_n$  has  $n$  zeros in the interval  $[-1, 1]$  and hence the higher-order terms in the approximation will be rapidly oscillating.

For physical problems in Fourier optics and antenna theory, for example, this behavior leads to high losses in the near field resulting in severe interference due to, e.g., plasma effects. The reader is referred, for example, to the exposition in Fante and Mayhan<sup>3</sup> for a discussion of the physical aspects of this problem. To avoid these difficulties, it is usually necessary to constrain the set of admissible solutions to an appropriate (compact) subset of a space of smoother functions to avoid excessive oscillations, and restore well-posedness. This is one of the earliest approaches to regularization by using *a priori* information about the class of admissible solutions (in this case compactness of the set of admissible solutions). See, for example, Ref. 22 and references cited therein to the work of Tikhonov.

The numerical approach based on collocation and finite difference approximations of the integral equation (1.2) leads to the matrix problem (1.1) or (1.5) in the 2D case. Take Eq. (1.1) as an example. Let  $c = -1$  in (1.2) and convert the interval  $[-1, 1]$  to  $[0, 2\pi]$  by setting  $t = \pi(x + 1)$ . Divide the interval  $[0, 2\pi]$  into  $N$  equidistant parts and set  $u_k = k\pi$ . Then Eq. (1.2) can be approximated by rectangular quadrature and collocation as

$$\frac{2}{N} \exp(iu_k) \sum_{j=0}^{N-1} \exp(-ikt_j) f\left(\frac{t_j}{\pi} - 1\right) = F(u_k),$$

$$k = 0, \dots, N - 1, \quad (\text{A1})$$

where  $t_j = j(2\pi/N)$ . Denote by  $f_j = f(t_j/\pi - 1)$  and  $F_k = (N/2)\cos u_k F(u_k)$ ; then Eq. (A1) leads to Eq. (1.1).

It is an intrinsic property of ill-posedness that any discretization of an ill-posed linear operator equation leads to a system of equations with the property that the inverse (or the generalized inverse) of the coefficient matrix is not uniformly bounded in  $N$ . But the inverse of the DFT matrix in Eq. (1.1) is uniformly bounded in  $N$ . There is no contradiction since the coefficient matrix of the system that arises from discretization of Eq. (1.2) is actually  $1/N$  times the ma-



Fig. 21. Reconstructions.

trix in Eq. (1.1). Irrespective of how one defines the coefficient matrix of the discretization of Eq. (1.2), the condition number of the discretized system tends to infinity as  $N$  tends to infinity. Recall that the condition number of the nonsingular system  $Ax = y$  is equal to the product of the norm of  $A$  and the norm of the inverse of  $A$ . Recall also that the row norm of a matrix is the maximum of the sums of moduli of elements in each row. It is easy to show that the row norm of the inverse coefficient matrix in Eq. (A1) is of order  $N$ , so it is not bounded in  $N$ . Since all matrix norms (or more generally all norms on a finite-dimensional space) are equivalent, the preceding statement is true irrespective of the norm used.

This numerical approach provides a practical scheme for resolving these difficulties and without the necessity to compute the eigenvectors of the integral operator. For example, Abdelmalek and Kasvand<sup>29</sup> discuss the Gauss LU decomposition of a discretized Fredholm system of Eq. (1.2) and a truncated LU decomposition is proposed; Abdelmalek *et al.*<sup>30</sup> utilize the Gauss-Jordan elimination of a regularized discretized Fredholm system of Eq. (1.2); Huang and Narendra<sup>31</sup> use the pseudoinverse characterized by SVD for restoring the noisy degraded images. Of course numerical difficulties and instability would still arise for very large-order matrices since the inverse or generalized inverse of the matrix is not uniformly bounded in  $N$  (or  $M$  and  $N$  for the case of a rectangular matrix). We resolve this problem by using the TSVD, which we are able to perform explicitly since we derive in this paper formulas for the singular values and singular vectors for any order  $N$  of the matrix.

We express our sincere thanks for the very helpful comments from the anonymous referees that led to the improved version of the paper. The research is sup-

ported by the China National Natural Science Foundation Youth Fund 10501051 and is also partially supported by National "973" Key Basic Research Developments Program G20000779.

## References

1. H. P. Baltes, *Inverse Source Problems in Optics* Vols. 9 and 10 of *Topics in Current Physics* (Springer, 1978 and 1980).
2. M. Z. Nashed, "Operator-theoretic and computational approaches to ill-posed problems with applications to antenna theory," *IEEE Trans. Antennas Propagat.* **AP-29**, 220–231 (1981).
3. R. L. Fante and J. T. Mayhan, "Bounds on the electric field outside a radiating system," *IEEE Trans. Antennas Propagat.* **AP-16**, 712–717 (1968).
4. R. L. Fante and J. T. Mayhan, "Bounds on the electric field outside a radiating system-II," *IEEE Trans. Antennas Propagat.* **AP-18**, 64–68 (1970).
5. J. B. Abbis, C. DeMol, and H. Dhadwal, "Regularized iterative and noniterative procedure for object restoration from experimental data," *Opt. Acta* **30**, 107–124 (1983).
6. R. N. Bracewell and S. J. Wernecke, "Image reconstruction over a finite field of view," *J. Opt. Soc. Am.* **65**, 1342–1347 (1975).
7. M. Bertero, C. DeMol, and G. A. Viano, "On the problem of object restoration and image extrapolation in optics," *J. Math. Phys.* **20**, 509–521 (1979).
8. J. M. Bertero, "Linear inverse and ill-posed problems," *Adv. Electron. Electron Phys.* **75**, 2–120 (1989).
9. J. M. Bertero, C. DeMol, and G. Viano, "The stability of inverse problems," in *Inverse Scattering Problems in Optics*, H. Baltes, ed., Vol. 20 of *Topics in Current Physics* (Springer, 1980), pp. 161–214.
10. R. J. Bell, *Introduction to Fourier Transform Spectroscopy* (Academic, 1972).
11. S. Kawata, K. Minami, and S. Minami, "Superresolution of Fourier transform spectroscopy data by the maximum entropy method," *Appl. Opt.* **22**, 3593–3598 (1983).
12. D. Slepian and H. O. Pollak, "Prolate spherical wave functions, Fourier analysis and uncertainty-I," *Bell Syst. Tech. J.* **40**, 43–64 (1961).
13. X. Hu, D. N. Levin, P. C. Lauterbur, and T. A. Spraggins, "SLIM: Spectral localization by imaging," *Magn. Reson. Med.* **8**, 314–322 (1988).
14. S. J. Reeves and L. P. Heck, "Selection of observations in signal reconstruction," *IEEE Trans. Signal Process.* **43**, 788–791 (1995).
15. A. K. Jain and S. Ranganath, "Extrapolation algorithms for discrete signals with application in spectral estimation," *IEEE Trans. Acoust. Speech Signal Process.* **ASSP-29**, 830–845 (1981).
16. B. J. Sullivan and B. Liu, "On the use of singular value decomposition and decimation in discrete-time band-limited signal extrapolation," *IEEE Trans. Acoust. Speech Signal Process.* **ASSP-32**, 1201–1212 (1984).
17. S. R. Degraaf, "SAR imaging via modern 2-D spectral estimation methods," *IEEE Trans. Image Process.* **17**, 729–761 (1998).
18. D. O. Walsh and P. A. Nielsen-Delaney, "Direct method for superresolution," *J. Opt. Soc. Am. A* **11**, 572–579 (1994).
19. D. J. Wingham, "The reconstruction of a band-limited function and its Fourier transform from a finite number of samples at arbitrary locations by singular value decomposition," *IEEE Trans. Signal Process.* **40**, 559–570 (1992).
20. M. Çetin and W. C. Karl, "Feature-enhanced synthetic aperture radar image formation based on nonquadratic regularization," *IEEE Trans. Image Process.* **10**, 623–631 (2001).
21. W. G. Carrara, R. S. Goodman, and R. M. Majewski, *Spotlight Synthetic Aperture Radar Signal Processing Algorithms* (Artech House, 1995).
22. J. Li and P. Stoica, "An adaptive filtering approach to spectral estimation and SAR imaging," *IEEE Trans. Signal Process.* **44**, 1469–1484 (1996).
23. M. Z. Nashed, *Generalized Inverses and Applications* (Academic, 1976).
24. C. L. Lawson and R. J. Hanson, *Solving Least Squares Problems* (Prentice-Hall, 1974).
25. B. Noble, "Methods for computing the Moore–Penrose generalized inverse and related matters," in *Generalized Inverses and Applications*, M. Z. Nashed, ed. (Academic, 1976), pp. 245–301.
26. G. H. Golub and C. F. Van Loan, *Matrix Computations*, 3rd ed. (Johns Hopkins University Press, 1996).
27. J. M. Varah, "On the numerical solution of ill-conditioned linear systems with application to ill-posed problems," *SIAM (Soc. Ind. Appl. Math.) J. Numer. Anal.* **10**, 549–565 (1973).
28. R. W. Gerchberg, "Super-resolution through energy reduction," *Opt. Acta* **21**, 709–720 (1974).
29. N. N. Abdelmalek and T. Kasvand, "Image restoration by Gauss LU decomposition," *Appl. Opt.* **18**, 1684–1686 (1979).
30. N. N. Abdelmalek, T. Kasvand, J. Olmstead, and M.-M. Tremblay, "Direct algorithm for digital image restoration," *Appl. Opt.* **20**, 4227–4233 (1981).
31. T. S. Huang and P. M. Narendra, "Image restoration by singular value decomposition," *Appl. Opt.* **14**, 2213–2216 (1975).